Chapter 4 Wind-Blown Sand Electrification

Many researchers were aware of that sand particles can charge up and they demonstrated that the electric field in sand (dust) storm is much stronger than the one of fair weather (Rudge 1913, 1914; Kunkel 1950; Latham 1964; Kamra 1969; Stow 1969). The charged sand particles and wind-blown sand electrification may affect wind-blown sand flow, which attract more attentions recently. In fact, sand charging and wind-blown sand electric field have significant effects upon the entrainment of sand particles, transportation and deposition, whereas, sand particles acquire substantial charges during their entrainments and collisions which conversely affect the wind-blown sand electric field. Besides, particles in an electric field are known to self-assemble into complex patterns (Sapozhnikov 2003). Clouds of charged dust regularly produce devastating explosions in particle and coal plants (Palmer 1973), and a calamitous blast can be occurred by a lot of charged particles. In exploring outer space, charged grit attaches itself to spacesuits and works its way into suit joints, causing them to leak air and so cut exploration time. Therefore, the studies on wind-blown sand electrification are expected to clarify these problems, to explore the mechanism of sand particles charged, and further to predict the effect of wind-blown sand electrification on the formation and evolution of the landforms on Mars. Back to Earth, the study of wind-blown sand electrification is meaningful to reveal how sand particles be entrained, transport and deposit in wind-blown sand flux, and to explore other planets successfully.

However, it is difficult to reveal how a sand particle becomes charge and what is the property of the electrical charges, especially in quantity. In addition, due to the limitations of the experiment instruments and methods, there are few studies on the experimental measure of wind-blown sand electric field and sand particles' charges.

The content of this chapter is arranged as follows, Sect. 4.1 reviews the existing studies on the phenomenon and mechanism of sand particles charging are introduced; Sects. 4.2 and 4.3 introduce the measurement results and theoretical prediction of wind-blown sand electric field, and finally Sect. 4.4 discusses the effect of wind-blown sand electrification on the entrainment of sand particles and propagation of electromagnetic wave in quantity. The effect of wind-blown sand electrification on the wind-

X. Zheng, *Mechanics of Wind-blown Sand Movements*, Environmental Science and Engineering,
DOI 10.1007/978-3-540-88254-1_4, © Springer-Verlag Berlin Heidelberg 2009

blown sand transportation and the theoretical prediction of dust devil will be discussed in next chapter.

4.1 Charged Sand Particles and their Charging Mechanisms

4.1.1 Observations and Measurements

Although electrical charges on sand particles have long been studied, researchers just argue how sand particles charge and their polarity. Rudge (1913) is one of the earliest researchers who studied sand charging, and he disrupted sand by means of an air jet and found that the large sand particles acquired positive charges and the air contained (or probably very small particles of sand suspended in the air) negative charges; Shaw (1929) blew sand through a sandpaper sheath at room temperature and found that the sandpaper became positively charged and the blown sand negatively charged. The charging was of the same sign but greater in magnitude when the temperature of the air was increased to 58 °C. Gill (1948) poured sand though a metal funnel and observed that smaller sand particles acquired positive charges and the larger ones acquired negative charges. By poured sand though a silica funnel, Peterson (1949) found that the sand acquired a negative charge. Since 1950s, many researchers begin to pay their attentions to a single sand particle's charge. Kunkel (1950) produced a puff of sand and measured the charge carried by individual particles. He found that although most particles were charged, the electrification was symmetrical, i.e., for each size range the total charge carried by the positively charged particles was equal to that carried by the negatively charged particles. From then on, many studies confirmed that sand particles can be electrified and the sign of the charge carried by a sand particle is relative to its size. For example, for quartz sand, Greeley and Leach's experimental (Greeley and Leach 1978) results showed that particles larger than 60 μm in diameter acquired negative charges, and particles smaller than 60 μm acquired positive charges, however, the critical diameter for the sign of charge is somewhat variable.

Since both sand and silt are tiny, it is quite difficult to measure the magnitude of charge carried by a single sand particle. Instead, many researchers measured the average charges of saltating sand particles such as the average charge-to-mass ratio. Using a sand trap to collect the sand particles, the average charge-to-mass ratio can be obtained by measuring the total charges and mass in the trap. For example, at Seminoe Reservoir (30 m

northeast of Rawlins, Wyoming), Schmidt et al. (1998) used Faraday-cage drift trap at 5 cm height and measured an average charge-to-mass ratio 60 $\mu C \cdot kg^{-1}$ and 150 μm average sieve diameter of collected in the trap.

Although we have got some results from the researches on wind-blown sand electrification, as mentioned above, it is far away from exploring this field. In fact, there are many factors which may affect the average charge-to-mass ratio of saltating sand particles, such as the sand diameter and wind velocity. In order to clarify the effect of these factors, we conducted electrification experiments in the field environmental wind tunnel of the Institute of Cold and Arid Regions Environmental Engineering of the Chinese Academy of Sciences. A D-Q3 digital amperemeter is used to measure the electric charges of sand particles by connecting the moustache of the amperemeter onto the surface of steel of the sand collector. In addition, the mass of collected sands in the collector chamber is weighted so as to determine the average charge-to-mass ratio, or the average charge per kilogram of sand, by dividing the measured charge with the measured mass. Experimental sands were sampled from the Tengger Desert, and the sand diameter ranges mainly in 40–600 μm whose distribution is shown in Fig. 4.1. Through sifting the 'mixed' sand with sieves of different aperture size, we got some 'uniform' sand samples to which the diameter distributes in a narrow band. Here, three 'uniform' sand samples with diameters of 0–75 μm, 100–150 μm and 500–1000 μm were employed. After starting wind tunnel, the charge-to-mass ratios are measured when the wind-blown

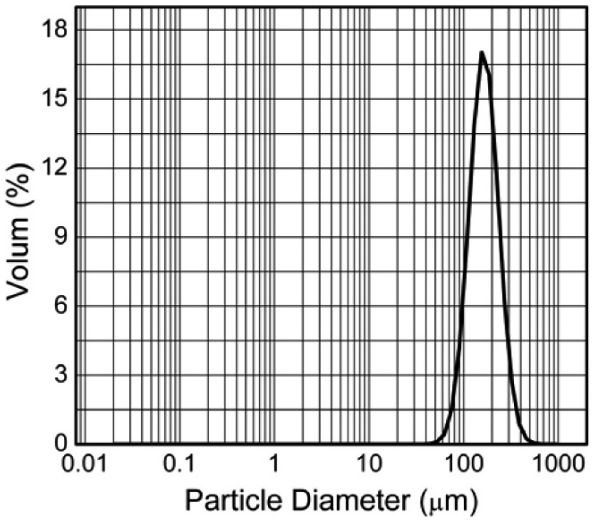

Fig. 4.1. Diameter distribution of sand particles used in wind tunnel experiments, which were sampled from the Tengger Desert (by the author et al.)

Table 4.1. Average charge-to-mass ratio for the 'uniform' sand measured under different wind velocities

Partical diameter [μm]	Wind velocity [m s^{-1}]	Charge-to-mass [μC kg^{-1}]
0–75	7	–124.5
0–75	15	–40.2
100–250	7	–64.2
100–250	15	–3.6
500–1000	10	0.95
500–1000	15	0.13

Table 4.2. Average charge-to-mass ratio for the 'mixed' sand under different wind velocities

Wind velocity [m s^{-1}]	Charge-to-mass [μC kg^{-1}]
7	–23.4
10	–19.3
15	–15.9
20	–9.8

Table 4.3. Variation of average charge-to-mass ratio for the 'mixed' sand with height under different wind velocities

Height [cm]	Wind velocity [m s^{-1}]	Charge-to-mass [μC kg^{-1}]
2–6	10	–24.5
2–6	20	–13.8
6–10	10	–125.0
6–10	20	–31.9
26–30	10	–330.0
26–30	20	–198.0
50–54	10	–1120.7
50–54	20	–890.2

sand flux is steady. For the three 'uniform' sand samples, the experiment is repeated to measure the average charge-to-mass ratio at different heights under different axial wind velocities. Tables 4.1 list some measured results of the average charge-to-mass for the three 'uniform' sand samples under three different axial wind velocities of 7 m·s^{-1}, 10 m·s^{-1}, and 15 m·s^{-1}.

From Tables 4.1–4.3, it can be found that sand particles saltate at the height of 0.02–0.54 m with each axial wind velocity; the sign of electric charge generated on the sands is mainly dependent upon the diameter of the sand particles, that is, when the diameter of the 'uniform' sand is less

than or equal to 250 μm, the charge is negative, whereas the sign is positive when the diameter is greater than or equal to 500 μm. In addition, results listed in Table 4.1 and Table 4.2 indicate that the magnitude of the charge-to-mass ratio for both the 'uniform' sand and the 'mixed' sand decreases with the axial wind velocity increasing, and increases with height for the 'mixed' sand. For the 'mixed' sand, a positive charge-to-mass ratio is measured when the axial wind velocity increases up to 20 $m \cdot s^{-1}$ as shown in Table 4.2, which is similar to the results given by Schmidt et al. (1998) as pointed out in the introduction.

4.1.2 Charging Mechanisms of Sand Particles

When the wind-blown sand electrification is confirmed by field or laboratory observations, people begin to pay an attention to the mechanisms of sand particles charged. Confined by the experiment instruments and measurement methods, up to now, it is still difficult to make quantitative measurements of sands charging procedure and there have no idea on measurements of magnitudes of charges acquired by a single sand particle. So the charging mechanism for sand particles is just a speculation. Latham is one of researchers who early tried to explain the charging procedure of sand particles. Earlier, Workan and Reynold (1948) investigated the mechanism of the thunder to observe that the ice acquires negative charges and the water droplet acquires positive charges after the water drip colliding with the ice. Their studies was based on the phenomenon of the snowstorm electrification, that is, smaller snow particles carry positive charges and larger snow particles carry negative charges. Similar to the mechanism of the thunder, Latham thought the asymmetric collision between large and small sand particles results in sand particles acquiring charges, and because of their smaller area of contact the small particles would become hotter than the larger ones. The temperature difference between the contact particles impels the charges' transfer, so the contact particles are charged. This explanation is so-called the temperature-gradient theory by Latham and Mason (1961). Later, Latham (1964) found that charge transfer drastically resulting from thermoelectricity when snow particles become coarser and the collision velocity is higher, which provided some experimental evidences for the temperature-gradient theory. However, we can not confirm the temperature-gradient theory directly because it is hard to measure the temperature difference and the magnitude of charge carried by particles with different diameters at the moment of collision. Even now, we can not learn more whether the temperature difference resulting from the collision between small sand particles can impels the charge transfer.

Besides Latham's work, there are many speculations and explanations to infer how the sand particles charged. Kanagy and Mann (1994) reviewed the seven mechanisms which have been recognized as potentially contributing to electrical charges on sand particles, that is: (1) Polarization by Earth's atmospheric electric field: Some researchers think that sand particles in atmospheric electric field, as a kind of dielectric material, will be polarized and the excess charges will be repulsed to the two sides of sand particles. Through collision among sand particles and breaking into small fragments, the particles are not neutral any more; (2) Triboelectric charging: that is to say two neutral sand particles will be charged by rubbing them. Ling et al. (1984) thinks that the electric field in sand (dust) storm is induced by sand particles, and those sand particles moves in anomalous trajectories and rub each another, maybe produce the charges, which is the triboelectrical phenomena; (3) Contact electrification: contact electrification generally involves two dissimilar materials which have come into contact and then are separated; (4) Cleavage/fractoelectrification: charges also may develop on sand particles as a result of cleavage or fracture; (5) Bombardment charging (photons; charging particles): sand particles will be charged due to solar wind bombardment or photoelectron ejection from sunlit surface; (6) Pyroelectric charging: when the crystal is heated is known as pyroelectricity, the charges will occur at the ends of a crystal; (7) Piezoelectric and electret effect charging: the crystal acquires charges when pressure is applied. The speculations (1), (5) and (7) indicate that sand particles can acquire charges even though they do not move, but through wind tunnel experimental results, it can be found that the magnitude of charges and the electric field are obviously variable when wind-blown sand transportation is stronger. So there is a relationship between the wind-blown sand electrification and sand transport. The speculations (1) and (5)–(7) maybe give a mechanism for sand particles charging, they are not the definitive one. Those speculations can not narrate why larger sand particles acquire the positive charges and the smaller ones acquire the negative charges when all those particles are acted upon the same actions such as polarization, pulverization, bombardment by solar ray, heating and piezoelectric charging. For the speculation (3), difference among the materials of sand particles at same place is hardly remarkable, so the probability for sand particles charging is little due to materials' difference, and further the speculation (4) is not appropriate. The speculation (2) agrees with the Latham's theory to some extent, if we deem the rubbing in speculation (2) as a result of collisions between particles with different diameters.

4.2 Measurements of Wind-Blown Sand Electric Field

4.2.1 Atmospheric Electric Field

The excess charges carried by atmosphere are the combination of several ions with opposite polarity. Observations indicate that there is downward electric field in the lower fair weather, which means that earth surface acquires the negative charges. In fact, atmosphere is a kind of weak electric material, and average density of current is 3×10^{-12} A·m^{-2} in fair weather. The density of surface charges delivered to the earth surface is about -10^{-9}C·m^{-2}, and the total charge is about -5×10^{5} C. For the simplicity, we usually let the electric field E_a of fair weather be negative. The direction and the magnitude of E_a around the world are almost equal everywhere, but E_a fluctuates slightly from time (place) to time (place). Usually, the electric field of fair weather is 120 V·m^{-1}, and it is 130 V·m^{-1} above sea level.

The electric field of fair weather decreases with height increasing, and reaches up to its maximum at ground level. From Gaussian theorem, the relationship of atmospheric electric field E_{a0} at ground level with the density of surface charges δ_e (C·m^{-2}) can be deduced, which is $E_{a0}=-4\pi\delta_e$. At the height 10 km, the atmospheric electric field is about 3% of E_{a0}. Due to the influence of buildings and the fluctuation of topography, the atmospheric electric field has a horizontal component, however, the effect of the building and topography on the atmospheric electric field can be ignored when one measures atmospheric electric field at a place 5 times higher than hill and building, and 3 times higher than slim building such as telegraphy pole (Fei et al. 2003).

Atmospheric electric field is related to the local atmosphere variation, because the local atmosphere variation can result in electric properties' variation of atmosphere such as the conductance and body charges, which determines the atmospheric electric field. At some terrestrial observation stations, two peaks of atmospheric electric field can be found that maximum values appear at 7:00–10:00 and 19:00–21:00 in local time while minimum values appear at 4:00–6:00 and 12:00–16:00. It can be found that the variations of atmospheric electric field are significant in the regions where the maximum electric field appears. For example the electric field increases from 70 V·m^{-1} to about 600 V·m^{-1} within 1 hour.

Furthermore, the atmospheric electric field is also related to the atmosphere pollutant. When the pollution is heavy, air conductance decreases and the atmospheric electric field increases rapidly. In ocean area, the arctic and Antarctic area, and some sparsely populated inland areas, the atmospheric electric field regularly varies in every day, and that is to say,

atmospheric electric field reaches up to its maximum at 18:00–19:00 and minimum at 4:00. Turbulence due to irons transport by air and thunderstorm also affects the atmospheric electric field. When the global thunderstorm is strongest, the atmospheric electric field reaches up to its maximum.

4.2.2 Field Observation of Wind-Blown Sand Electric Field

Rudge (1913) measured the atmospheric electric field in South African by electrometer, during an ordinary fine weather day, a dusty day and a very dusty day. He found that sand (dust) storm could increase the electric field and strong sand (dust) storm could completely modify the direction of electric field, which verified the observation by Michie Smith in India. In addition, Rudge found the electric field can reach up to 10 $kV \cdot m^{-1}$ (let downward be positive, henceforth). From then on, many researchers investigated the wind-blown sand electric field, and they found the electric field is fluctuant and is relate to wind velocity, temperature, relative humidity and observation site (Kamra 1972; Qu 2003). Kamra (1972) measured the atmospheric electric field and wind-blown sand electric field at many places near a desert of the southwestern states. He found that wind velocity, especially the turbulent component of wind velocity, has a great effect on the wind-blown sand electric field. Such puffs and whirls of dust caused by wind gusts often produce stronger electrical perturbation which last for

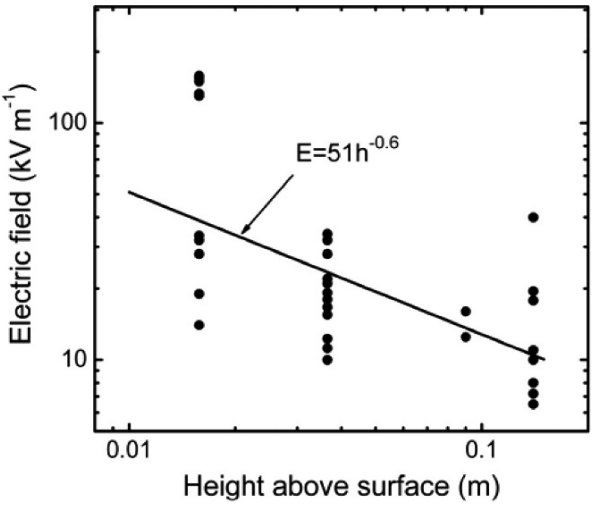

Fig. 4.2. Measurements of wind-blown sand electric field and its fit curve, where the average wind velocity is 7.0 $m \cdot s^{-1}$ at 1.5 m height (from Schmidt et al. 1998)

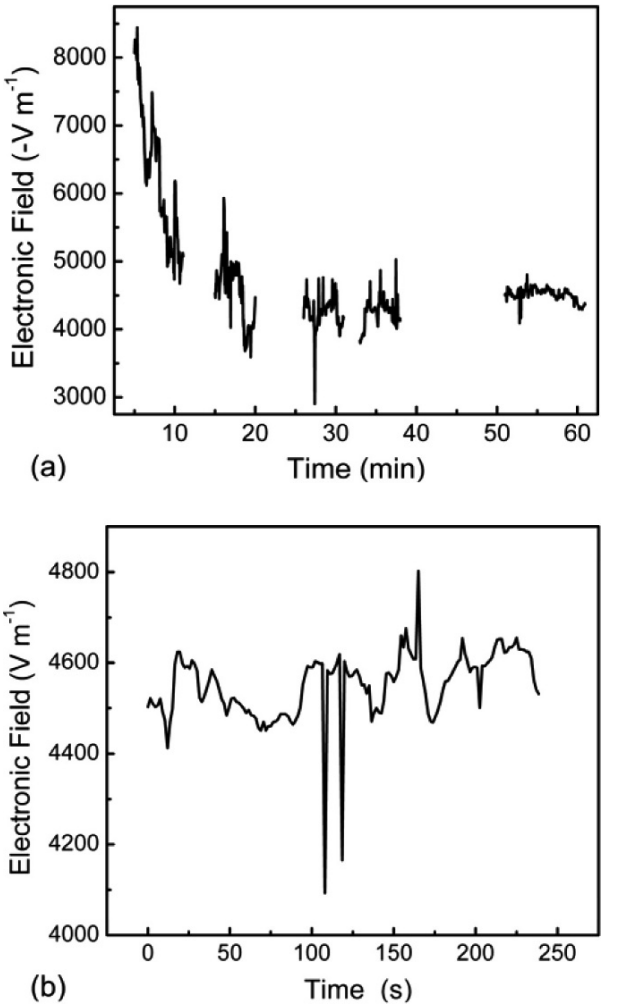

Fig. 4.3. Profile of electric field measured on the top of a building in Lanzhou University, at the height about 60 m, **(a)** record time is 16:05–16:54 and **(b)** record time is 16:50–16:54 (by the author et al.)

a few minutes, and their frequency depends on the gustiness of wind. Schmidt et al. (1998) measured the wind-blown sand electric field above a sand dune, and he found that the electric field decreased rapidly with the height above the sand dune surface, became zero at about 20 cm and approached to the fair-weather field above 2 m. The electric field measurements for the region 1.73–20 cm are shown as Fig. 4.2. From the Fig.4.2, it can be found that electric field exponentially decreases with and increasing

of height and we fitted a power-law profile below 15cm under a condition that the average wind velocity is 7.0 $m \cdot s^{-1}$ at 1.5 m height.

In a sand (dust) storm, the electric field becomes stronger near the building in the center of city. In March 9th, 2003, we measured the electric field

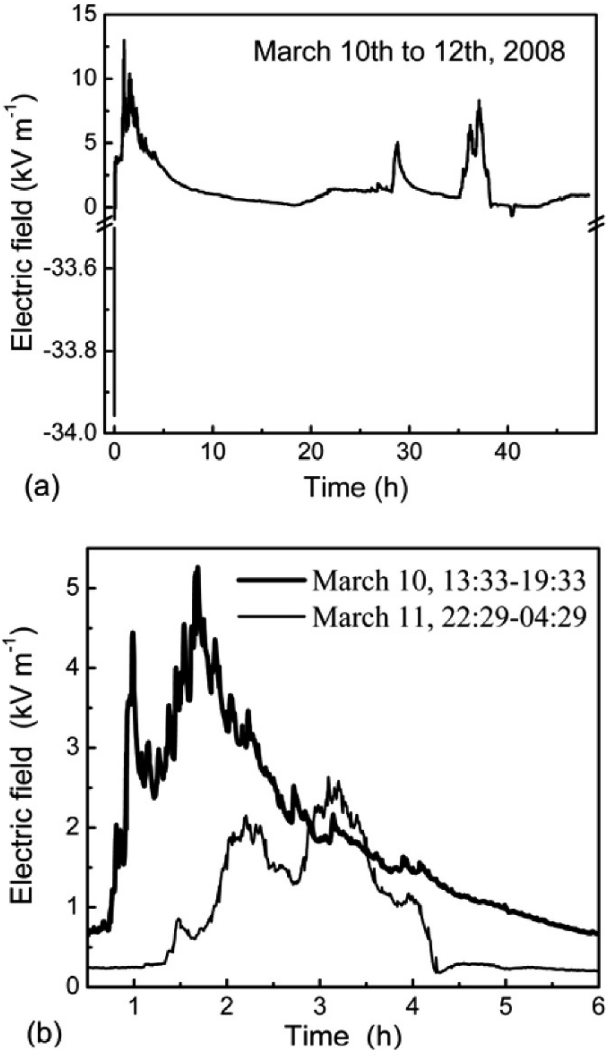

Fig. 4.4. Profile of electric field near a sand dune measured in the Badain Jaran Desert during March 10th to 12th, 2008 with sampling frequency 1 Hz; **(a)** the electric filed during the whole record time; **(b)** the wind-blown sand electric field during two dusty weather conditions, which are the amplificatory images of results in the circles of **(a)** (by the author et al.)

at the top of a building in Lanzhou University which is in the center of Lanzhou city. The electrical field is measured at a height of 60 m when a sand (dust) storm happened and the visibility was 800 m. The wind-blown sand electric could reach up to 8 $kV \cdot m^{-1}$, and it was about 4.5 $kV \cdot m^{-1}$ even the sand (dust) storm becomes weak (see Fig. 4.3a). From Fig. 4.3b, it can also be found that the electric field is very unstable.

Wind-blown sand electric field is related to the temperature and humidity. We measure the electric field and its variation with temperature and humidity near a sand dune in the Badain Jaran Desert during March 10th to 12th, 2008. Fig. 4.4 shows the measurement results of electric field from March 9th to 12th, 2008, with the sampling frequency is 1 Hz. Fortunately, during our measurement, we experienced two sand storms, so we measured the electric field of two dusty weather. One sand (dust) storm happened in the afternoon of March 10th, 2008 with low wind velocity, about 10 $m \cdot s^{-1}$, and the other sand (dust) storm happened in deep night of March 11th, 2008 with the stronger wind 17.0 $m \cdot s^{-1}$. Sand particles can be blown away from earth surface about 30 cm during the first storm and almost dry sand particles were blown away during the second one. The electric fields during the two sand (dust) storms are shown in the Fig. 4.4a and we marked them in red circle lines for well distinguishing. It is noteworthy that temperature in the afternoon of March 10th, 2008 is lower than the one at night of March 11th, 2008, with a difference about 12 °C, and humidity of the former is higher than the one of latter, about 60% difference. The electric field of former is weaker than the latter. In order to distinguish them, we plot the electric field serials in Fig. 4.4b during two dusty weather conditions, which indicate that the temperature and humidity have an effect on the wind-blown sand electric field. In addition, our measurement shows that the electric field periodically varies with the same period as the one of temperature and humidity.

4.2.3 Wind Tunnel Measurement of Wind-Blown Sand Electric Field

It is first time that the author et al. investigated the electric field in wind tunnel (Zheng et al. 1998; 2000), and measured the electric field of the 'uniform' wind-blown sand flux and the 'mixed' wind-blown sand flux shown as Fig. 4.5. It can be found that the wind-blown sand electric field (named by E_z), perpendicularly to the earth surface, is opposite to the electric field of fair weather. Fig. 4.5a, the wind-blown sand electric field decreases with the height increasing, where the electric field holds its absolute value. For the 'uniform' wind-blown sand flux, the electric field

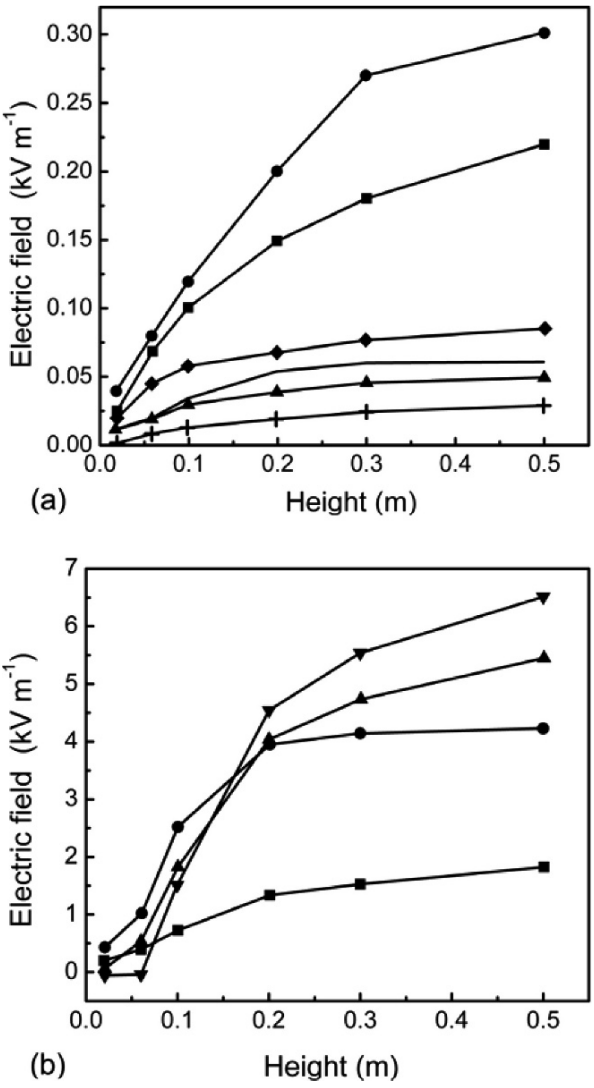

Fig. 4.5. Wind-blown sand electric field versus height **(a)** for the 'uniform' wind-blown sand flux, and **(b)** for the 'mixed' wind-blown sand flux; There are six results for 'uniform' wind-blown sand flux, –■– the results for the wind velocity u_{ax} = 7 m·s^{-1} and D_s = 0–75 μm, –●– the results for the wind velocity u_{ax}= 15 m·s^{-1} and D_s = 0–75 μm, –▲– the results for u_{ax} = 7 m·s^{-1} and D_s =100–250 μm, –◆– the results for the wind velocity u_{ax} = 15 m·s^{-1} and D_s =100–250 μm; –+– the results for u_{ax} = 10 m·s^{-1} and D_s =500–1000 μm, —— the results for u_{ax} = 20 m·s^{-1} and D_s =500–1000 μm; There are four results for the 'mixed' wind-blown sand flux, and –■–, –●–, –▲– and –▼– are results for the wind velocity 7 m·s^{-1}, 10 m·s^{-1}, 15 m·s^{-1} and 20 m·s^{-1}, respectively (from Zheng et al. 2000)

increases with the particles diameter increasing and also increases withwind velocity increasing (see Fig. 4.5a). The variation of electric field with wind velocity is complex for the mixed wind-blown sand flux, especially near the earth surface (see Fig. 4.5b). Comparison of electric field of

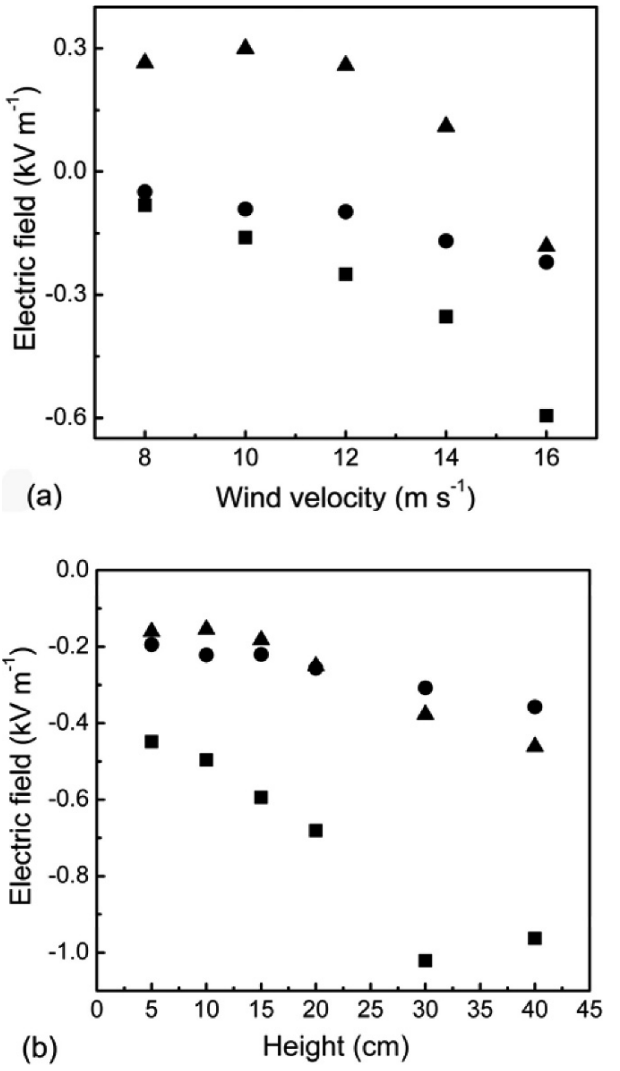

Fig. 4.6. The electric field vary with **(a)** wind velocity and **(b)** height; ■ horizontal electric field E_x; ● lateral electric field E_y; ▲ vertical electric field E_z (measured by the author et al in the Multi-function environmental wind tunnel of Lanzhou University)

mixed wind-blown sand flux with one of 'uniform' wind-blown sand flux, it can be found that the former is much higher than the latter, and at the wind velocity 20 $m \cdot s^{-1}$, the maximum of the former is 20 times of the latter.

It is known that the electric field is a vector, but there are few works reported on its other components (E_x and E_y). Here, we let E_x be parallel to the axes of wind tunnel and opposite to the wind direction, and E_y be perpendicular to the both E_x and E_z. Though E_x and E_y are far lower than the wind-blown sand field E_z (see Fig. 4.6), they can reach up to 0.2 $kV \cdot m^{-1}$ in the 'mixed' wind-blown sand flux, which is higher than the fair weather electric field. From Fig. 4.6, it can be found that E_x and E_y decrease with height or wind velocity increasing. Fig. 4.7 shows that both $|E_x / E_z|$ and $|E_y / E_z|$ rapidly increase with the increase of wind velocity for wind velocity lower than 14.0 $m \cdot s^{-1}$. For wind velocities higher than 14.0 $m \cdot s^{-1}$, $|E_x / E_z| > 0.8$ and $|E_y / E_z| > 0.85$. At any height, there is a critical wind velocity, and when wind velocity is higher than the critical value, $|E_x / E_z|$ and $|E_y / E_z|$ are larger than 1, which indicate that E_x and E_y are stronger than E_z. In addition, E_x is larger than E_y under a certain wind velocities and heights. Of course, we need to verify if the wind tunnel results can simulate the one of field, it is maybe necessary to consider the effect of wind tunnel's scale on the wind-blown sand electric field.

In order to describe the relationship between E_x and E_z, the E_y and E_z, we fit $|E_x/E_z|$ and $|E_y/E_z|$ as an exponent-law profile and a linear-law profile, respectively. At the same time, they are functions of wind velocity and height as follows,

$$\left|E_x / E_z\right| = a_x \exp\left(\frac{u_{ax}}{b_x}\right) + c_x , \tag{4.1}$$

$$\left|E_y / E_z\right| = a_y u_{ax} + b_y , \tag{4.2}$$

where u_{ax} is the axial wind velocity in the wind tunnel and its dimension is $m \cdot s^{-1}$.

$$\begin{aligned} a_x &= -0.0283 + 0.0092h - 3.665 \times 10^{-4} h^2 , \\ b_x &= 1.6044 + 0.2769h - 0.0106h^2 , \\ c_x &= 0.2936 - 0.0604h + 0.0028h^2 , \\ a_y &= -0.4189 - 0.1422h + 0.0065h^2 , \\ b_y &= 0.0151 + 0.0302h - 0.0015h^2 . \end{aligned} \tag{4.3}$$

and h is the height above the sand bed with dimension cm.

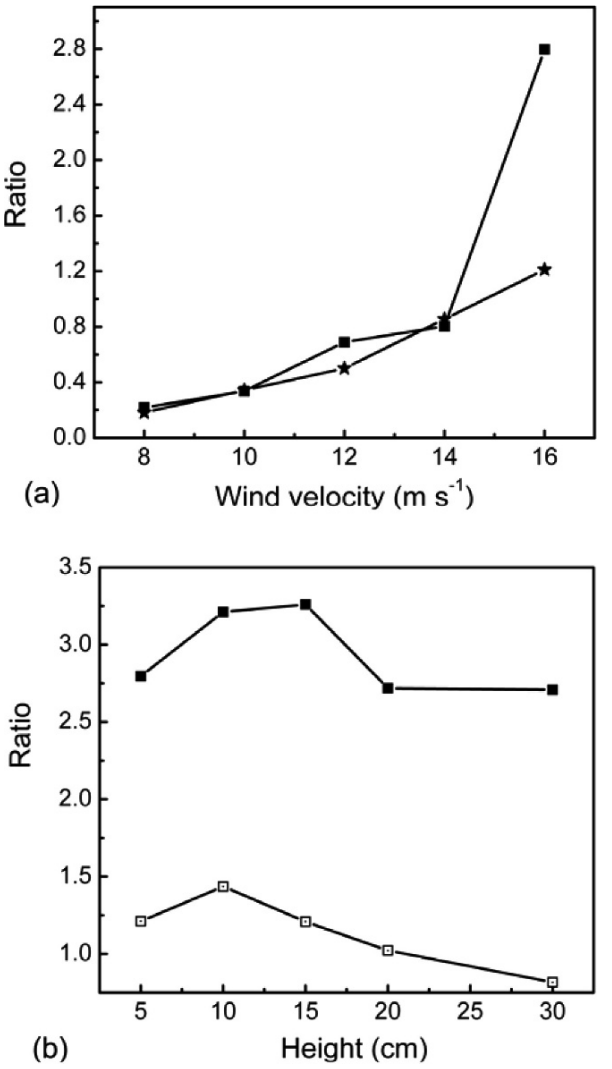

Fig. 4.7. Ratio of horizontal electric field to vertical electric field $|E_x / E_z|$ (–■–) and ratio of lateral electric field to vertical electric field $|E_y / E_z|$ (–□–), vary with **(a)** wind velocity and **(b)** height (measured by the author et al. in the Multi-function environmental wind tunnel of Lanzhou University)

4.3 Theoretical Calculation of Wind-Blown Sand Electric Field

Zheng et al. (2004) derived a formula to calculate the wind-blown sand electric field. Shown in Fig. 4.8, let the surface of sand bed as *xOy*-plane, and the *x* coincides with the wind direction and *z* is perpendicular to the *xOy*-plane. Assuming that the sand bed is infinite, we need only consider the effects of the charged particles enclosed within the rectangular with sides $2a \times 2b$, and centered at the projection of the point *P* to be observed in the *xOy*-plane.

Without loss of generality, we located coordinate system in such a way that the point *P* lies on the *z* axis with coordinate $P(0, 0, z)$. Then the horizontal component of the electric force at the point *P* produced by a charged particle located at (x', y', z') is equal in magnitude and opposite in direction to that produced by one at $(x', -y', -z')$, and they will cancel each other out. Therefore the electric field has only a vertical component, and that is the vertical component of wind-blown sand electric field, namely E_z.

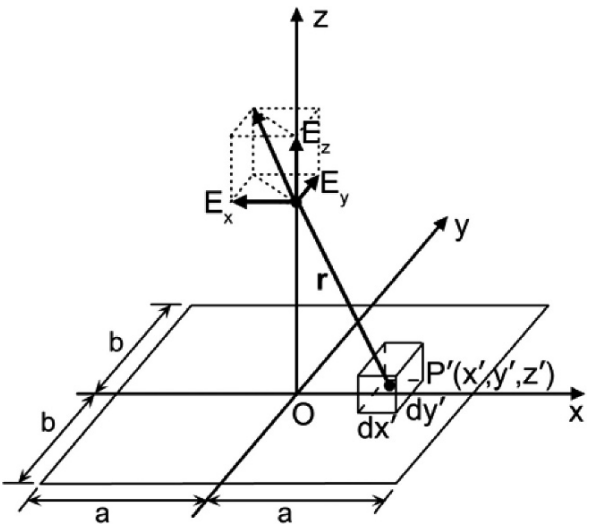

Fig. 4.8. Schematic of electric field, including horizontal component E_x, lateral component E_y and vertical component E_z., produced by a point charge at the point $P'(x', y', z')$ (from Zheng et al. 2004)

4.3.1 Electric Field Due to Sand Particles Moving in Air

When wind-blown sand flux is at steady state, the distribution of the sand particles ejected from the sand bed and accelerated by the wind just reproduces itself after impacting the bed, which means the numbers of ejected and impacting sand particles are approximately equal to each other. Thus the number density of the particles N (i.e., the number of moving particles per unit volume) in the windblown sand flux may be assumed to vary only with the height over the sand bed, i.e., $N = N(z)$. Then, the distribution of electric charges of saltating or suspending sand particles could be described by the volume charge density $\rho_q(z)$, which is given by

$$\rho_q(z) = \frac{1}{6}\pi\rho_s D_s^3(z) N(z) C_q(z). \tag{4.4}$$

Where $D_s(z)$ and $C_q(z)$ are the particle diameter and the charge-to-mass ratio respectively. ρ_s is the particle density. It is noteworthy to point that usually $D_s(z)$ and $C_q(z)$ are not constants in real wind-blown sand flux, but for simplicity, here we let $D_s(z) = D_s$ and $C_q(z) = C_q$.

Consider a differential volume $dx'dy'dz'$ in the wind-blown sand flux as shown in Fig. 4.8. It contains a distribution of electric charges characterized by a volume charge $\rho_q(z')dx'dy'dz'$. According to Coulomb's law (Frankle, 1986), the differential electric field dE_{zs} at a point $P(0, 0, z)$ due to a differential amount of charge $\rho_q(z')dx'dy'dz'$ contained in the volume $dx'dy'dz'$ is given by

$$dE_{sz} = \frac{\rho_q(z')dx'dy'dz'}{4\pi\varepsilon_0 r^3}\mathbf{r} = \frac{\rho_s C_q D_s^3 N(z')dx'dy'dz'}{24\varepsilon_0 r^3}\mathbf{r}. \tag{4.5}$$

Where ε_0 (= 8.85×10^{-12} $C^2N^{-1}m^{-2}$) is the electrical permittivity of air and $\mathbf{r}$ is the vector from the point P' to point P with magnitude $r = \sqrt{x'^2 + y'^2 + z'^2}$. By applying the principle of linear superposition, the total electric field can be obtained by integrating the fields produced by all the charges making up the charge distribution. Thus

$$E_{sz} = \frac{\rho_s C_q D_s^3}{6\varepsilon_0}\int_{z_0}^{\infty} \mathrm{sign}(z-z')N(z')\arcsin\frac{ab}{\sqrt{\left[a^2+(z'-z)^2\right]\left[b^2+(z'-z)^2\right]}}dz'. \tag{4.6}$$

Where z_0 is the aerodynamic roughness related to the surface property. When $z = z'$, $\mathrm{sign}(z-z') = 0$, and when $z > z'$ and $z < z'$, $\mathrm{sign}(z-z') = 1$ and $\mathrm{sign}(z-z') = -1$, respectively. It is seen from Eq. 4.6 that the electric field intensity depends mainly on the number density of the charged particles in

the wind-blown sand flux. Generally, the number density $N(z)$ changes not only with the height, but also with the movement of sand particles. Let $N_1(z)$ and $N_2(z)$ respectively represent the number densities for saltating and suspending sand particles, then the electric field produced by saltating particles, E_{sz}^1, and that produced by suspending ones, E_{sz}^2, can be obtained.

Based on the assumption that all saltating and suspending sand particles carry negative charges, form Eq. 4.6, we can find that the electric field at height z produced by saltating sand particles or suspending sand particles lower than height z is downward and increases with height increasing, whether z lies in the saltation layer, the suspending layer or the layer above of the suspending layer. The electric field at height z produced by saltating sand particles or suspending sand particles higher than height z is upward and decreases with height increasing. So the direction of the electric field produced by saltating and suspending sand particles is opposite to the electric field of fair weather and it is upward. This electric field decreases with height increasing, and there exists a height z' and $E_{sz'}^1 = 0$ or $E_{sz'}^2 = 0$. The electric field is opposite to the atmospheric electric field, when $z > z'$, the electric field is inverted with a same direction as the one of fair weather electric field, and it increased with height increasing. When electric field reaches up its extremum and it will decrease with height increasing. $E_{sz} \to 0$ when $z \to \infty$. We can also find that both the electric field E_{sz}^1 produced by saltating sand particles and the electric field E_{sz}^2 produced by suspending sand particles make the wind-blown sand electric field stronger or weaker, but their strengths are not equal due to the difference of volume number of saltating sand particles from the one of suspending sand particles.

4.3.2 Electric Field Due to Sand Particles in Sand Bed

Assuming the charge's distribution across a surface, which is characterized by the surface charge density σ_q, the total charges of the particles on the surface and those in the air should be zero according to the law of conservation of electric charge (Frankle 1986). Thus

$$\int_{-a}^{a}\int_{-b}^{b}\sigma_q d\mathrm{x}'dy' + \int_{-a}^{a}\int_{-b}^{b}\int_{z_0}^{\infty}\rho_{q1}(z')d\mathrm{x}'dy'dz' + \int_{-a}^{a}\int_{-b}^{b}\int_{z_0}^{\infty}\rho_{q2}(z')d\mathrm{x}'dy'dz' = 0 . \quad (4.7)$$

Where $\rho_{q1}(z)$ and $\rho_{q2}(z)$ are the volume charge densities of saltating and suspending sand particles respectively. We can get

$$\sigma_q = -\frac{1}{6}\pi\rho_s C_q D_s^3 \left[\int_{z_0}^{\infty} N_1(z')dz' + \int_{z_0}^{\infty} N_2(z')dz'\right]. \quad (4.8)$$

The electric field produced by sand particles in sand bed can be written:

$$E_{cz} = -\frac{\rho_s C_q D_s^3}{6\varepsilon_0}\left[\int_{z_0}^{\infty} N_1(z')dz' + \int_{z_0}^{\infty} N_2(z')dz'\right]\arcsin\left(\frac{a}{\sqrt{a^2+z^2}}\frac{b}{\sqrt{b^2+z^2}}\right). \quad (4.9)$$

It is obvious that charges carried by sand particles in sand bed are positive when we let saltating and suspending sand particles acquire negative charges. So the electric field produced by sand particles in sand bed is downward and decreases with height increasing, that is to say if $z \to \infty$, $E_{cz} = 0$.

4.3.3 Total Electric Field Due to Charged Sand Particles in Wind-Blown Sand Flux

Considering the electric field of fair weather, the real electric field produced by charged sand particles is $E_z = E_a + E_{sz}^1 + E_{sz}^2 + E_{cz}$. Here we take $E_a = -0.1$ kV·m^{-1} and sign '–' is opposite to z. As we know, the volumetric concentration of the suspending sand particles is only about 10^{-8}–10^{-6} (Anderson and Hallet 1986), which is much less than the transport rate generated by saltating particles approximating 75% in the wind-blown sand flux (Bagnold 1941). That is $N_2(z) << N_1(z)$. Therefore the electric field produced by suspending sand particles is usually neglected.

The complete profiles of the electric field produced by charged particles in wind-blown sand flux at different wind velocities are respectively plotted in Fig. 4.9a for the height $z \leq 0.02$ m and in Fig. 4.9b for $z \geq 0.02$ m, where the friction wind velocities are 0.3 m·s^{-1}, 0.5 m·s^{-1} and 0.78 m·s^{-1}, respectively. It could be seen in Fig. 4.9 that the variations of the electric field does not always monotonically increase or decrease with the height. In fact, the profile of the electric field is composed of three layers. In the first layer near the bed, the electric field can reach several hundred kilovolts per meter in magnitude directed upward, and decreases quickly to zero with height increasing. In the second layer, i.e., after the field becomes zero, the direction of the electric field changes from upward to downward, which is the same as that of the fair weather's electric field, and the magnitude of the electric field intensity increases from zero to an order of several kilovolts per meter within 10–20 cm. The third layer is the upper one in which the direction of the electric field is also the same as that of the fair weather field and the magnitude of the field decreases as the height reaches until it is equal to that of the fair weather field. This finding coincides well with the phenomena described by Schmidt et al. (1998).

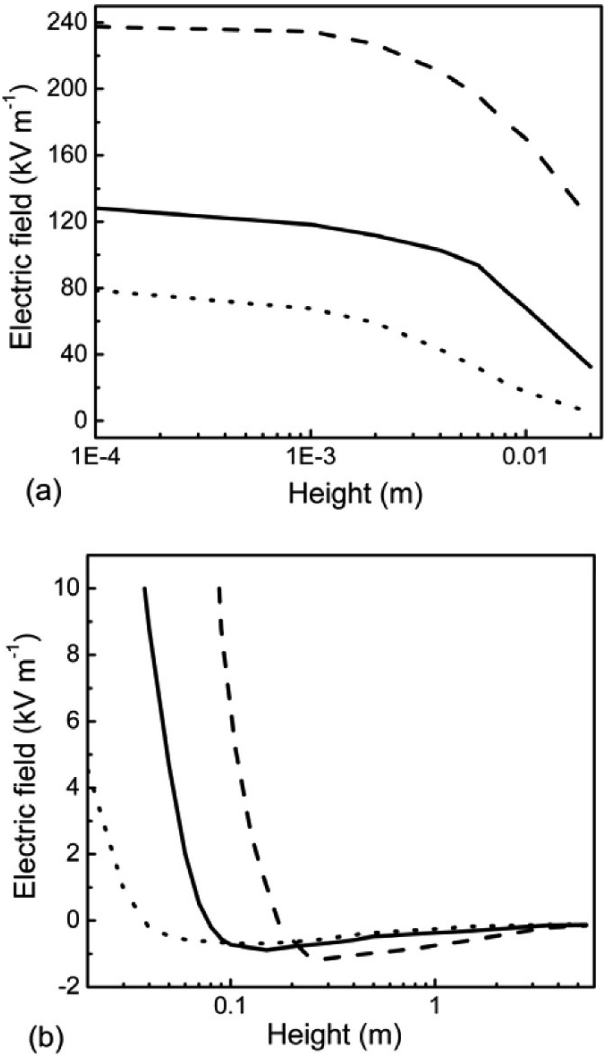

Fig. 4.9. Profile of electric field produced by all charged sand particles in wind-blown sand flux (D_s = 0.25 mm, C_q = –60 μC·kg^{-1}); (a) for 0.0001 m≤z≤0.02 m; (b) for z≥0.02 m; – – – for u_* = 0.78 m·s^{-1}, —— for u_* = 0.50 m·s^{-1} and - - - - for u_* = 0.30 m·s^{-1} (from Zheng et al. 2004)

Ignoring E_{sz}^2 and E_{cz}, we can get the electric field produced by only saltating sand particles (see Fig.4.10). From Fig.4.10, the profile of electric field produced by charged saltating sand particles also display a structure of three layers, and the variation of the electric field in each layer is same as the one of the electric field produced by all charged sand particles. In

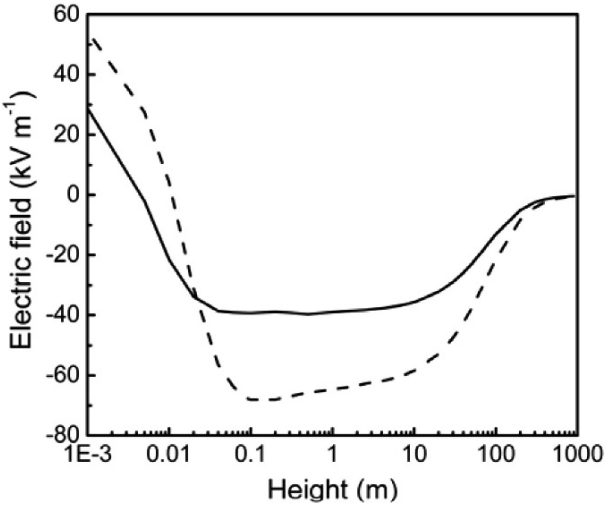

Fig. 4.10. Profile of the electric field produced by charged saltating sand particles in wind-blown sand flux with different charge-to-mass ($C_q = -60$ μC·kg^{-1}, $D_s = 0.25$ mm), —— the results for $u_* = 0.30$ m·s^{-1}; – – – – the results for $u_* = 0.50$ m·s^{-1} (modified from Zheng et al. 2004)

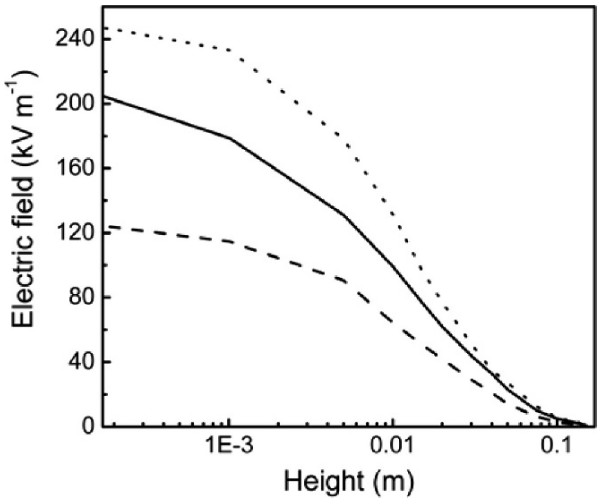

Fig. 4.11. Profile of the electric field produced by all charged sand particles in wind-blown sand flux with different charge-to-mass ($u_* = 0.69$ m·s^{-1}, $D_s = 0.25$ mm), – – – – for $C_q = -90$ μC·kg^{-1}; ——for $C_q = -60$ μC kg^{-1} and - - - - for $C_q = -30$ μC kg^{-1} (modified from Zheng et al. 2004)

addition, we find that electric field indeed increases within a height, which agrees with the measurement results by Zheng, et al. (2003), and the electric field produced by only saltating sand particles also is affected by the particle diameter and wind velocity.

From Eqs. 4.7 and 4.9, it is obviously that the charges carried by sand particles have an effect on the wind-blown sand electric field, and Fig. 4.11 shows the wind electric field varies with height when friction wind velocity is $0.7 m \cdot s^{-1}$ and the charge-to-mass is $-90\ \mu C \cdot kg^{-1}$, $-60\ \mu C \cdot kg^{-1}$ and $-30\ \mu C \cdot kg^{-1}$ respectively. Near the earth surface ($z < 5$ cm), the charge-to-mass has a significant effect on the electric field, and the larger of charge-to-mass, the stronger of electric field at the same height. With height increasing, the charge-to-mass has a little effect on the field, and the wind-blown sand electric field approaches to the fair weather's electric field.

Friction wind velocity also has an effect on the wind-blown sand electric field. Shown as Fig. 4.9b, before the wind-blown sand electric field approaches to the fair weather's electric field, the wind-blown sand electric field increases with the friction wind velocity increasing.

It is noteworthy to point that the mass flux is also affected by the wind-blown sand electric field, which will be discussed in next chapter. Recently, some work is conducted to simulate the wind-blown sand electric field following the idea mentioned above, Zheng et al. (2004) and Kok et al. (2006, 2008) take the charges transfer during particle-bed collision and sand particles start acted by wind-blown sand electric field into account. But Kok et al. (2006, 2008) didn't display the simulation results of the wind-blown sand electric field.

4.4 Effects of Charged Sand Particles

4.4.1 Effects on the Entrainment of Sand Particles'

Earth's surface is generally a good conductor because soil particles are usually covered by a thin, conducting film of water (Kanagy and Mann 1994). Therefore, the atmospheric electric field or external electric field can induce charges at the surface (Wahlin 1986). It is the first time that Yue et al. (2003) conducted a study on the threshold wind velocity of an irregular sand particle subjected to electrostatic force, and they also considered the effect of the eccentric distance, eccentric angle and particle diameter. They find that wind-blown sand electric filed indeed has an effect on the threshold wind velocity. Especially for a relative high field, it greatly decreases the threshold wind velocity of sand particles.

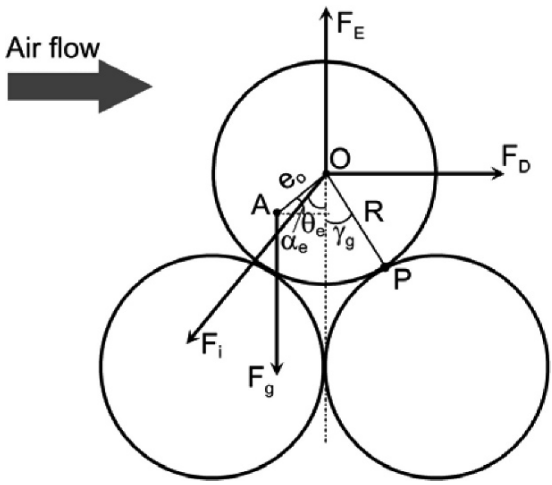

Fig. 4.12. A Schematic illustration of a packed form of sand particles in sand bed, and e_o, α_e and γ_g are the eccentricity, eccentricity-angle and the angle between inter-particle force and gravity, respectively; Point A and O are the center of mass and center of geometry of the sand particle. Point P is the start point of the sand particle. F_i, F_D, F_E and F_g are the inter-particle force, drag force, electrostatic force and gravity

Kok and Renno (2006) analyzed the sand lift acting upon the gravitation, inter-particle force and electric force, considering sand particles charged under the external electric field. With the aid of experiments, Kok and Renno deduced (2008) the threshold electric field necessary to lift a particle under the windless condition. It can be found the critical electric field strength firstly decreases and then increases with sand particle diameter increasing. When the electric field exceeds 150 kV·m^{-1}, a sand particle can be directly uplifted from surface. They also confirmed that the wind-blown sand electric field can reduce the threshold friction velocity by providing an additional upward force.

In addition, a sand particle in sand bed is always packed by other sand particles (see Fig.4.12), so its entrainment is confined by its neighboring sand particles. Considering the gravity, inter-particle force, drag force and electrostatic force, we can deduce the threshold friction velocity for a sand particle as

$$u_{*_t}^2 = \frac{1}{A_1\rho}\cos\gamma_g\left[\frac{g\pi D_s}{6}(\rho_s-\rho)\left(\sin\gamma_g+\frac{e_o}{R}\cos\alpha_e\right)+\frac{A_2}{D_s}\sin(\theta_e+\gamma_g)-\frac{1.37\pi\varepsilon_0 E_z^2}{C_s}\sin\gamma_g\right]. \quad (4.10)$$

Where E_z is the total field. C_s is a scaling constant introduced to account for the non-sphericity of solid particles (C_s = 0.4761), A_1 and A_2 are

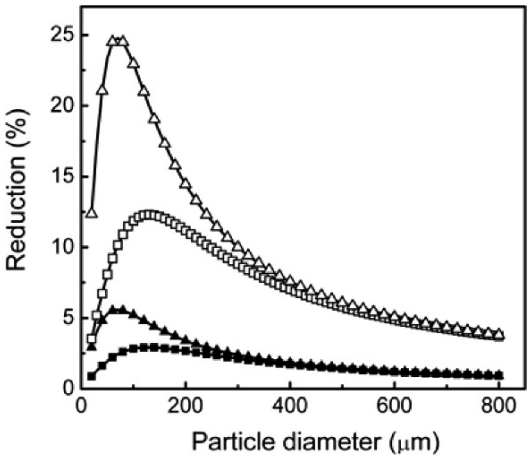

Fig. 4.13. Reduction of the threshold friction velocity as a function of particle diameter, wind-blown sand electric field and packed form; –■– the results under the electric field 50 kV·m^{-1} for $\gamma_g = 2°$, $\theta_e = 1°$; –▲– the results under the electric field 50 kV·m^{-1} for $\gamma_g = 85°$, $\theta_e = 70°$; –□– the results under the electric field 100 k·Vm^{-1} for $\gamma_g = 2°$, $\theta_e = 1°$; –△– the results under the electric field 100 k·Vm^{-1} for $\gamma_g = 85°$, $\theta_e = 70°$ (by the author et al.)

dimensionless empirical coefficients associated with the aerodynamic drag and inter-particle force, and they are 4 and 1.5×10^{-4} kg·s^{-2}, respectively. e_o and α_e are the eccentricity and eccentricity-angle (see Fig. 4.12). θ_e and γ_g are angles between inter-particle force and gravity, and line of *OP* to gravity. From Eq. 4.10, it can be found that the threshold friction velocity decreases under the wind electric field, and it also can be found that the percent reduction of the threshold friction velocity are effected by the particle diameter, the wind-blown sand electric field and the packed form. Given a packed form, the percent reduction varies with the particle diameter shown as Fig.4.13, and the threshold friction velocity can fall 25% when the wind-blown sand electric field is about 100 kV·m^{-1}.

4.4.2 Effects on Electromagnetic Wave Propagation

The attenuation of microwaves in sand (dust) storm is directly observed by Al-Hafid et al. (1979a, 1979b, 1980) and Chen (1991). They found that the sand (dust) storm not only has an effect on the attenuation of electromagnetic wave propagation, for example, the microwaves of 10 GHz weakened at a velocity 10–15 dB per tens of minutes, in a sand (dust) storm occurring in Nasiriya-Daraji, but also, to some bad extent, the microwaves

can be completely weakened within several hours. The attenuation of electromagnetic waves is relative to the sand particles radius, and for the electromagnetic waves of 10 GHz, the attenuation reaches up to maximum when the wave length is comparative to the particle radius.

Based on the scattering theory of millimeter microwaves and Rayleigh approximation, Ryde (1941) is the earliest researcher who calculated the scatter of microwaves propagating in a sand (dust) storm. Haddad et al. (1983) measured the permittivity and diameter distribution of sand particles collected from a sand (dust) storm happened in Iraq, and then they calculated the attenuation of microwaves of 9.4 GHz propagating in a sand (dust) storm by the relationship of optical visibility and dust concentration presented by Chu (1974), which is 0.001 $dB \cdot m^{-1}$ for the sand particles with mass density 6×10^{-5} $g \cdot cm^{-3}$. In order to verify the calculation results, Haddad measured an attenuation of 0.0034 $dB \cdot m^{-1}$ under the same condition as one in calculation, and it is as much as 34 times larger than the calculated value, which shows that the effect of a sand (dust) storm on electromagnetic wave propagation is notable.

Zhou et al. (2005) presented a new model to investigate the effect of charges carried by sand particles on attenuation of electromagnetic waves. For simplicity, they took a sand particle as a sphere with the permittivity ε_s and the volume V_s, and the electrical charges uniformly distribute in the shape of a spherical cap as shown in Fig. 4.14. In real sand (dust) storms,

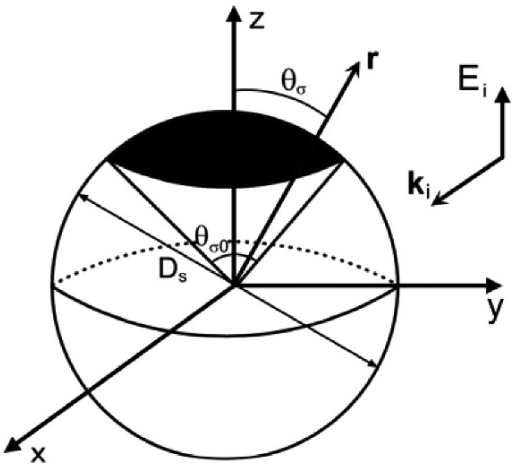

Fig. 4.14. Schematic drawing of a sand particle with the electric charges distributed on a spherical cap (marked by the black domain) with angle $\theta_{\sigma 0}$ and density of surface charge σ_q, and $\mathbf{k}_i$ and $\mathbf{E}_i$ are incident direction of the incident electromagnetic wave and incident E-field direction, respectively

the radius of a sand particle is far smaller than the wavelength of centimeter microwaves or millimeter microwaves, so we can use the Rayleigh approximation to solve the inner electric field of the particles.

Eq. 4.7 gives an analytical formula of the scattering attenuation(denoted by A) when a microwave with wave number k propagates in a sand (dust) storm which has a visibility V_b and average sand particle with a partial distribution of electric charges σ_q and $\theta_{\sigma 0}$, and derivation of formula is reported by Zhou et al. (2005) for details.

$$A=\frac{20}{V_b}k^4 D_s^4\left|\frac{\varepsilon_s-\varepsilon_0}{\varepsilon_s+2\varepsilon_0}\right|^2+\frac{90}{V_b}D_s k\varepsilon_r''\left|\frac{\varepsilon_0}{\varepsilon_s+2\varepsilon_0}\right|^2+\frac{7.5}{9}k^4 D_s^6 C_q{}^2\frac{\rho_s^2(\varepsilon_s-\varepsilon_0)^2\sin^2\theta_{\sigma 0}}{\varepsilon_0^4 E_i^2(1-\cos\theta_0)^2 V_b}. \quad (4.11)$$

Where ε_r'' is the relative permittivity of sand particles to air. E_i is the electric field of incident electromagnetic wave.

Characteristic curves of the attenuation coefficient varying with angle $\theta_{\sigma 0}$ of electric charge distribution for different densities of surface charge σ_q shown as Fig. 4.15, in order to compare them with the measured results by Haddadt et al. (1983). Here the same parameters as ones in the real sand (dust) storm are used, such as frequency 9.4 GHz, radius of sand 40 μm, permittivity of sand 2.634 + 0.734i, visibility 10 m and the intensity of incident electric field 50 V·m^{-1}. The measured value of attenuation coefficient in this experiment is 0.034 dB·m^{-1} (Haddad 1983), which is plotted

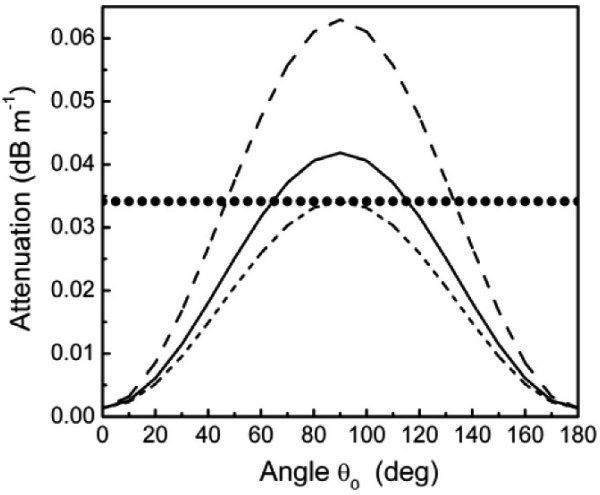

Fig. 4.15. Characteristic curves of the attenuation coefficient varying with angle $\theta_{\sigma 0}$ of electric charge distribution for different densities of surface charge σ_q; – – – for σ_q = 2.7 μC·m^{-2}, —— for σ_q = 3.0 μC·m^{-2} and - - - - for σ_q = 3.7 μC·m^{-2}. Measured value, ● attenuation coefficient A = 0.034 dB·m^{-1} (from Zhou et al. 2005)

by a straight line parallel to the horizontal axis in Fig. 4.2. When the sand particles are not charged, the attenuations are 0.001 $dB \cdot m^{-1}$, which is equal to the one calculated by Haddadt (1983). From Fig. 4.15, it can be found that the attenuation coefficient varies with the increase of $\theta_{\sigma 0}$ in a sinusoidal curve, given the charge-to-mass ratios. When $\theta_{\sigma 0} = 0$ and $\theta_{\sigma 0} = \pi$, the attenuation coefficient is minimum, and $\theta_{\sigma 0} = \pi / 2$, the attenuation coefficient reaches up to its maximum value. That is to say that the charges carried by sand particles have a significant effect on the attenuation of electromagnetic waves. When $\sigma_s = 2.7$ $\mu C \cdot m^{-2}$ and $\sigma_s = 3$ $\mu C \cdot m^{-2}$, the attenuation coefficients are equal to the measured one, accordingly $\theta_{\sigma 0} = 63°$ and $\theta_{\sigma 0} = 117°$. It also indicates that the sand particles are partly charged. And an important conclusion can be induced that sand particles are charged partly.

Though we can solve the problem mentioned above by Mie theory (Bohren and Huffman 1983) when the size of dust particles is not smaller than the wavelength of electromagnetic waves, it is necessary to consider the effect of sand particles' velocity and multiple-scattering among sand particles on the attenuation of electromagnetic waves. So it requires a further study.